

Active foundering of a continental arc root beneath the southern Sierra Nevada, California

George Zandt*, Hersh Gilbert*, Thomas J. Owens†, Mihai Ducea*, Jason Saleeby‡ & Craig H. Jones§

**University of Arizona, Department of Geosciences, Tucson, Arizona 85721, USA*

†University of South Carolina, Department of Geological Sciences, Chapel Hill, North Carolina 29208, USA

‡California Institute of Technology, Department of Geological and Planetary Sciences, Pasadena, California 91125, USA

§University of Colorado, Department of Geological Sciences, Boulder, Colorado 80309, USA

Seismic data provide unique images of crust-mantle interactions during ongoing removal of the dense batholithic root beneath the southern Sierra Nevada. The removal was initiated between 10 and 3 Ma with a Rayleigh–Taylor-type instability, but with a pronounced asymmetric flow into a mantle downwelling (drip) beneath the adjacent Great Valley. A nearly horizontal bottom-to-the-SW shear zone accommodated the detachment of the ultramafic root from its granitoid batholith. With continuing flow into the mantle drip, viscous drag at the base of the remaining ~35-km-thick crust has thickened it by ~7 km in a narrow crustal welt beneath the western flank of the range. Adjacent to the welt and at the top of the drip, a V-shaped cone of crust is being dragged down tens of kilometres into the core of the mantle drip, causing the disappearance of the Moho in the seismic images. Viscous coupling between the crust and mantle is driving present-day surface subsidence.

Giant magmatic bodies, or batholiths, that constitute nearly the entire crust in belts thousands of kilometers long are integral features of major mountain systems associated with continental arcs. There is a growing recognition that the growth of ~30-km-thick granitoid batholiths must involve a two-step magmatic differentiation process that generates an equal or even greater thickness of ultramafic residual roots beneath the granitic bodies (e.g., ref. 1). Removal of such dense ultramafic roots is often cited as a mechanism for differentiation in Cordilleran arcs (e.g., refs 2, 3) to produce the overall intermediate composition of the continents^{4,5}, but the actual timing and mechanism of removal, and whether all such roots eventually founder, remains uncertain. In southern California, a compelling case has been made for a late Cenozoic (<10 Ma) foundering event beneath the southern Sierra Nevada batholith⁶⁻¹⁰. We present new seismic results that provide direct evidence connecting crustal structures associated with the removal event to the mantle downwelling imaged in previous tomography studies¹¹⁻¹³ (see supporting materials). Analyses of receiver functions reveal seismic anisotropy at the base of the crust that may be related to shearing along a detachment zone that became a new crust-mantle boundary. Viscous drag at the base of the remaining ~35-km-thick crust has thickened it by ~7 km in a narrow crustal welt, and at the top of the drip, a V-shaped cone of crust is being dragged down tens of kilometres into the core of the mantle drip.

Crustal welts and missing Moho

A 20-station, 1997 PASSCAL experiment and five permanent stations in the Caltech network in this area recorded the teleseismic data used in this study (Fig. 1). The 25 stations encompass the southern Sierra Nevada region, where xenoliths from Miocene, Pliocene, and Quaternary volcanic fields document the presence of an ultramafic root in the Miocene (~10 Ma) and its absence in the Pliocene (~3 Ma)⁶⁻⁸. Residual garnet pyroxenite xenoliths found in mid-Miocene volcanic rocks from the Sierra Nevada⁶ are

extremely dense rocks ($3.5\text{--}3.6\text{ g cm}^{-3}$) compared with typical mantle peridotites ($\sim 3,300\text{ kg m}^{-3}$) due to their garnet- and Fe-rich nature⁴. This heavy residue is prone to separation from its overlying low-density granitoid batholith and eventual convective foundering into the mantle. A pulse of small-volume, high-potassium volcanism that erupted within a circular area about 200 km in diameter centered just south of Long Valley (Fig. 1) has been suggested to indicate both the locality and timing of the main removal event in the southern Sierra Nevada^{14,15}. This might represent only part of the area where the root was removed, as 3–4 Ma volcanism extends much farther north and south¹⁶.

Receiver function seismology uses seismic waves produced by *P*- to *S*-wave mode conversions generated below seismic stations to image intracrustal and upper-mantle interfaces. Like reflection seismology, receiver functions are seismic traces that can be migrated to depth and geographically stacked to make pseudo-cross sections of the subsurface in which the depths of continuous horizons, such as the Moho, can be identified and mapped. We stacked receiver functions calculated from teleseismic recordings in common conversion area bins (e.g., refs 17–19). A crustal thickness map based on contouring the Moho *P*-to-*s*-converted phase (*Ps*) reveals a complex pattern of thickness variations in the Sierra Nevada and surrounding regions (Fig. 1). Beneath the northeastern corner of the study area, which includes the Big Pine volcanic field, the crustal thickness is about 36 km, 7–8 km thicker than the crust in Owens Valley farther south. The crust thickens westward, forming a crustal welt with a maximum thickness of 42 km beneath the Kings volcanic field. The Moho changes to a very different character south of the area of the high-potassium volcanism, where the crust in the Sierra Nevada is almost everywhere less than 36–37 km thick. Under Owens Valley and adjacent ranges to the east, the Moho is relatively flat at ~ 30 km.

The pattern of crustal thickness variations determined from receiver functions agrees well with the results from seismic refraction studies²⁰. In particular, both indicate thicker crust (~40 km) beneath the Sierra Nevada north of about 36.5° latitude. The main difference between the two models these methods produce is that the refraction model shows a bulge of thicker crust (~35 km) beneath the Owens Valley extending from south of Big Pine to about 36° latitude that is absent in the receiver function Moho-depth model (~30 km). Our crustal thicknesses are also in good agreement with an independent receiver function study done with the permanent stations in the Caltech network that overlap our study area²¹.

Three NE-SW receiver function cross sections are shown in Fig. 2 with interpretations overlain to highlight some interesting details of the crustal structure. The Moho is a large-amplitude, positive-polarity (red) arrival at depths between 30 and 42 km. In the southern cross section (A-A') the Moho is a smooth interface, deepening gradually to the west, where the amplitude diminishes abruptly beneath the Great Valley. In the middle cross section (B-B') the Moho arrival disappears farther east beneath the western edge of the range. In the northern cross section (C-C') the Moho arrival is more complex, exhibiting an echelon offsets before disappearing even farther east beneath the western foothills. An absence of a clear wide-angle Moho reflection (*PmP*) from this portion of the crust was noted in the active source experiments, but it was attributed to noisy recording conditions in the Great Valley^{13,20}. In contrast, all the broadband stations were located on outcrop sites, and examination of data from the six stations sampling the region of absent Moho, some of which extend well into the western flank of the range, show the disappearance is not due to interference from basin-generated noise.

The missing Moho in the western foothills (Fig. 1) has two possible explanations. One scenario is that the shear velocity contrast at the Moho is significantly

reduced by a localized low- V_s zone in the uppermost mantle, perhaps due to serpentinization of the mantle like that found in active forearc regions²². This is a plausible explanation given that this region was within the forearc region of a subduction zone during much of the Cenozoic, although not an active one for the past ~ 20 Ma. An alternative explanation is that small-scale topography on the Moho is scattering away the coherent Ps conversion, as well as the active source *PmP* reflections. Later, we present synthetic modelling and additional independent evidence that supports this latter explanation.

Anisotropy in the lower crust

Another prominent feature in the cross sections is a series of three en echelon negative-polarity arrivals (blue) observed in the mid- to lower crust (at depths of ~ 20 - 30 km) throughout the study region (Fig. 2). This feature corresponds to the mid-crustal negative-polarity arrival (MCN) imaged by Jones and Phinney²³ based on data from several small arrays deployed in an earlier study (MK, HM, and DP00 in Fig. 1). In the southern part of the study area, the top of this feature under Owens Valley is at a depth of ~ 20 km. Moving westward into the range, there appears to be a ~ 8 - 10 km en echelon step downward of the negative-polarity phase beneath the Sierra Nevada (A-A'). This 25-km-deep arrival underlies the entire high Sierra within the study area. Farther north (B-B') the en echelon offset occurs beneath the eastern edge of the range. In the northern section where the crust thickens to a maximum of ~ 42 km, the thickening appears to occur in an en echelon fashion accompanied by another negative-polarity phase at ~ 35 km depth (C-C').

Analysis of directional variations in the negative-polarity arrival (MCN) on the radial receiver function and its associated arrival on the tangential receiver function suggests the presence of an anisotropic layer at the base of the crust composed of an east-dipping fabric. The seismic anisotropy of this fabric is characterized by a slow

direction perpendicular to the layering and equally fast directions in all orientations within the plane of the layering. One example of the azimuthal variations that results from the presence of anisotropy is displayed in the radial and tangential receiver functions for station JUN shown in the supporting materials. We find that in comparing various models to data from our stations that models with a planar fabric striking N-S to NW-SE and dipping at some amount greater than $\sim 45^\circ$ downward to the E or SE provide the best fit to our data. Azimuthally varying patterns similar to those shown in the supporting materials are found at most stations located in the Sierra Nevada and adjacent ranges across Owens Valley. Stations showing either different patterns or little evidence for crustal anisotropy are largely located within or near the edge of the Moho 'hole', near the eastern front of the Sierra Nevada, or south of latitude 36°N where the root was removed earlier (Fig. 1).

Resolution tests

The common-conversion-point stacking technique employed here assumes that the *P*-to-*S*-converted phases are produced by laterally continuous horizontal structures and does not account for focusing or diffraction effects resulting from dipping or laterally varying interfaces. Images presented here display a dip on the Moho as well as negatively polarized arrivals that appear as a series of en echelon steps. We test the veracity of these images by determining whether or not we are able to resolve features with dips or steps with coarsely spaced stations. These tests are performed by computing synthetic receiver functions using a finite-difference algorithm (O. Boyd, personal communication, 2004) for various structures and then processing the synthetics in the same way as the data. The station spacing and incidence angles of events in the synthetic tests are chosen to reflect those of the actual data. First, the presence of a structural cusp on the Moho was modelled to see how such a structure would appear in receiver function stacks (Fig. 3, top plot labeled 'Cusp'). The size of the cusp (50 km

wide by 25 km deep) was made to be similar to the volume of crustal material entrained into the mantle by ‘the drip’ as it appears in the cross sections and based loosely on published numerical models (e.g., ref. 9). This is the feature responsible for creating the observed ‘hole’ in the Moho. In the cusp model significantly diminished amplitude arrivals are observed centered over the cusp, demonstrating that a cusp-shaped feature can produce the observed Moho hole. No clear arrivals off the sides of the cusp were seen. The dipping edges of the cusp are too steep to be imaged here, but energy does arrive at the base of the cusp. The tests demonstrate that a V-shaped notch of crust ~50-km-wide by ~25-km deep, cut into the mantle, is sufficient to make the Moho disappear in the receiver function stack. This is the basis for the ‘V’-shaped Moho holes interpreted in the cross sections of Fig. 2. The western edge of the hole is poorly constrained due to the absence of stations in the Great Valley. We also tested a series of models with a dipping Moho overlain by an en-echelon low-velocity zone with vertical offsets of varying magnitude (see supplementary materials). We found that with our station spacing en-echelon steps offset by at least 5 km can be recovered, while smaller steps can appear as a continuously dipping layer. Additionally, the continuously dipping LVZ does not become aliased into a series of steps.

Alignment of crustal welt, Moho hole, and mantle drip

The structural features and fabric of the crust we have imaged do not correlate in any simple way with Sierran topography or geology. However, a revealing clue to the significance of these patterns is the alignment of major features along a SW trend from near Bishop to Visalia (Fig. 1). Along this trend are the center of the region of potassic volcanism, the crustal welt beneath the Kings volcanic field, the Moho hole beneath the adjacent foothills, the center of the surface projection of the mantle drip, and the Tulare dry lakebed. The final clue that provides a connection among all these features is the recognition of a subsiding sub-basin in the Great Valley centered above the mantle

anomaly²⁴. The locus of subsidence can be observed in the drainage patterns in the southern Sierra Nevada where rivers discharging into the valley north of Fresno flow northward, while those within the circle of influence of the drip flow into the Tulare internal drainage basin (Fig. 1). Ongoing work reconstructing sedimentation patterns suggests that the local sub-basin began forming at ~3–4 Ma and that it has migrated southwest to its current position²². These observations can be connected to an active southwest-migrating convective instability. The alignment of features in the Sierra Nevada and the absence of similar features to the west suggest a strong asymmetry to the process. The localized crustal welt beneath the Kings volcanic field may reflect viscous drag at the base of the crust in the wake of southwest mantle motion (e.g., refs 23–28). Numerical models of analogous convective instabilities^{29,30} show that at the point of downward detachment of the lithosphere, the lower crust will be entrained several tens of kilometers or more into the downward flow, providing an explanation for the V-shaped Moho hole. The surface expression of the crustal foundering would be an elliptical zone of subsidence produced by viscous coupling between the downwelling drip and the overlying crust³¹.

We believe the anisotropic fabrics observed near the crust-mantle boundary are associated with a shear zone between the crust and the foundering root. Well-developed shear zones generally have fabrics that are parallel to the shear zone, whereas fabrics or layering at an oblique angle to the shear plane are usually associated with the initial stages of shearing under brittle-ductile conditions³². The observed anisotropy could be due either to alignment of slow-axis minerals, such as mica, or to fluid- or melt-filled cracks in planes perpendicular to the axis direction. In both cases the planes containing the minerals or cracks dip E to NE. The distinction between these two origins for the anisotropy is important because they predict opposite sense of shear with the same alignment (see supplementary materials). The preferred interpretation is that the dipping fabric is related to fluid- or melt-filled fractures or veins formed during the initial stage

of shearing. Cracks, fractures, or veins formed during shearing will align in a direction antithetic to the shear direction; hence such features would be consistent with bottom-to-the-west shear. Laboratory experiments on feldspars at high temperatures and large shear strains showed melt segregated into melt-rich bands oriented obliquely to the shear plane and antithetic to the shear deformation³³. Fluids or melts are generally required to open and propagate fractures at these depths. (We know that at least some existed because even the limited Sierra Nevada volcanism brought up xenoliths from such depths.) This interpretation requires high temperatures to trigger dehydration reactions or melting to induce fracturing. Although low temperatures are usually associated with convective instabilities^{34,35}, the formation of a shear zone between heterogeneous media can produce significant viscous heating³⁶. Even without shear heating, the rapid thinning of the lithosphere associated with asymmetric instabilities may be sufficient to locally raise mantle temperatures significantly. Quaternary volcanism, xenolith geothermometry, and magnetotelluric measurements suggest the relatively recent attainment of high Moho temperatures ($\sim 1000^{\circ}\text{C}$), at least beneath Owens Valley^{7,8,37}. In an alternative interpretation that the anisotropy is due to oriented micas, the fabric is probably controlled by the development of an S-C fabric. In this case, the observed orientation of the anisotropy indicates top-to-the-west shear³², the opposite sense of the root moving westward into the drip (top-to-the-east sense of shear) but possibly consistent with an earlier phase of extension, suggesting a two-stage evolution involving a reversal in the sense of slip (see supplementary materials).

Destabilization, detachment, and sinking

Combining the new seismic results with the existing geologic constraints, we suggest the following sequence of events in the southern Sierra Nevada (Fig. 4). A dense root originated as an ultramafic phase of Sierran batholith formation during Mesozoic subduction. The Cretaceous granitic batholith and its garnet- and pyroxene-rich root

formed a strong microplate under the influence of a cool geotherm that initiated during Laramide flat-slab subduction and is still reflected in modern heat flow (e.g., ref. 38) and geothermometry (e.g., refs 6, 39, 40). A number of factors could have played a role in destabilizing the root in the late Cenozoic. Several events all occurred in short order in the early Miocene that probably contributed to the demise of the ultramafic root. First, the volcanic arc returned to the northern Sierra (Fig. 4a), just within and north of the area pictured in Fig. 1 (ref. 41), terminating any unusually cool temperatures at the base of the continental lithosphere and possibly fluxing the Sierran lithosphere. Second, the Mendocino triple junction passed through this region between 10 and 20 Ma, exposing the Sierran lithosphere to the asthenosphere of the 'slab window' (Fig. 4b)⁴² and changing the basal stresses on the root¹¹. Third, extensional faults rooted into the Sierran crust developed starting at ~15 Ma (e.g., ref. 34), weakening the top of the ultramafic root⁴³.

Although we have no direct information on the critical initial stages of the removal process, we suggest a history consistent with numerical models of lithospheric deformation in which the mechanical lithosphere (including the root) deforms by localized strain in the upper region in conjunction with Rayleigh–Taylor-type viscous deformation in the lower portion³⁰ (Fig. 4c). As the instability grew, a pronounced asymmetry in the foundering developed, resulting in a concentrated downwelling under the San Joaquin Valley and western foothills of the Sierra Nevada accompanied by a more widespread mantle upwelling under the western Basin and Range and easternmost Sierra (Fig. 4d). During this latter stage of development, the downwelling created a region of strong convergence in the mantle while the crust remained in a state of extension, suggesting decoupling (or a weak shear zone) between the crust and mantle except where the flow turns downward.

One explanation for the westward location of the downwelling is that the convective instability was initiated on the western edge of the batholith due to compositional variations¹⁰, but a change in the initiation location alone does not explain the asymmetric nature of the ensuing instability. Another explanation is that the instability was initially centered under the main crest of the Sierra but was displaced westward by asthenospheric flow related to the mantle wind⁴⁴ or to westward influx of asthenosphere into the slab window, a flow direction controlled by the shape and polarity of the paleo-subduction zone^{45,46}.

Numerical modeling of detachment of a lithospheric root that incorporates brittle crustal rheologies demonstrates that asymmetric formation of a convective instability is possible only if a prescribed dipping shear zone²⁴ or a laterally limited zone of weak brittle rheology is present²⁹. The hydrated lithosphere just east of the Sierra Nevada presumably established in the early Cenozoic above the subducting Juan de Fuca plate⁴⁷ is a likely location for such a laterally limited weak zone, especially given the initiation of extension in this region starting at ~15 Ma (e.g., ref. 34). Westward motion of the detaching root would draw in weakened North American-affinity mantle from beneath the adjacent Basin and Range. Small-volume partial melting of this lithosphere mantle can reasonably explain the high-potassium, low- ϵ_{Nd} volcanism that occurred in the Sierra Nevada during the Pliocene¹⁵. Another important consequence of the asymmetric geometry of the removal process is the implication that the separation of the batholith from its root occurred along a concentrated zone of simple shear at the present-day Moho.

An important question that remains unanswered is how much of the North American Cordilleran magmatic arc developed and then lost an ultramafic root? It is still debated whether the entire Sierra Nevada formed and lost its root^{44,48} or whether the removal is progressing northward and only the southern Sierra root is sinking, with the

root remaining intact or in a nascent drip stage under the northern Sierra Nevada. The tectonic environment is obviously important in determining whether and when root removal occurs, but more documented examples are needed to clarify these relationships. Although not the focus of this paper, root foundering has important tectonic and geomorphic consequences, e.g., collapse of the Salinian-Mohave block⁴⁸, uplift of the Sierra Nevada and its influence on adjacent ranges and faults¹⁶, and localized subsidence²⁵. Root removal is an important tectonic process with global implications, not only in terms of long-term crustal compositional evolution, but also in providing insights on lower-crustal deformation mechanisms, continental strength, and influence on regional tectonics.

References

1. Ducea, M. N. The California arc: Thick granitic batholiths, eclogitic residues, lithospheric-scale thrusting, and magmatic flare-ups. *GSA Today* **11**, 4–10 (2001).
2. Kay, R. W. & Kay, S. M. Creation and destruction of lower continental crust, *Geologische Rundschau*, **80**(2), 259–278 (1991).
3. Kay, R. W. & Kay, S. M. Delamination and delamination magmatism. *Tectonophysics* **219**, 177–189 (1993).
4. Ducea, M. N. Constraints on the bulk composition and root foundering rates of continental arcs: A California arc perspective. *J. Geophys. Res.* **107**(B11), 2304, DOI 10.1029/2001JB000643 (2002).
5. Jull, M. & Kelemen, P. B. On the conditions for lower crustal convective instability. *J. Geophys. Res.* **106**(B4), 6423–6446 (2001).
6. Ducea, M. N. & Saleeby, J. B. Buoyancy sources for a large, unrooted mountain range, the Sierra Nevada, California: Evidence from xenolith thermobarometry. *J. Geophys. Res.* **101**, 8229–8244 (1996).

7. Ducea, M. N. & Saleeby, J. B. A case for delamination of the deep batholithic crust beneath the Sierra Nevada, California. *Int. Geol. Rev.* **40**, 78–93 (1998).
8. Ducea, M. N. & Saleeby, J. B. The age and origin of a thick mafic-ultramafic keel from beneath the Sierra Nevada batholith. *Contrib. Min. Petrol.* **133**(1-2), 169–185 (1998).
9. Wernicke, B. *et al.* Origin of high mountains in the continents: The Southern Sierra Nevada. *Science* **271**, 190–193 (1996).
10. Saleeby, J., Ducea, M. & Clemens-Knott, D. Production and loss of high-density batholithic root—Sierra Nevada, California. *Tectonics* **22**(6), 1064, DOI 10.1029/2002TC001374 (2003).
11. Zandt, G. & Carrigan, C. R. Small-scale convective instability and upper mantle viscosity under California. *Science* **261**, 460–463 (1993).
12. Jones, C. H., Kanamori H. & Roecker, S. W. Missing roots and mantle “drips”: Regional P_n and teleseismic arrival times in the southern Sierra Nevada and vicinity, California. *J. Geophys. Res.* **99**, 4567–4601 (1994).
13. Ruppert, S., Fliedner, M. & Zandt, G. Thin crust and active upper mantle beneath the Southern Sierra Nevada in the western United States. *Tectonophysics* **286**, 237–252 (1998).
14. Manley, C. R., Glazner, A. F. & Farmer, G. L. Timing of volcanism in the Sierra Nevada of California: Evidence for Pliocene delamination of the batholithic root? *Geology* **28**, 811–814 (2000).
15. Farmer, G. L., Glazner, A. F. & Manley, C. Did lithospheric delamination trigger late Cenozoic potassic volcanism in the Sierra Nevada, California? *Geol. Soc. Am. Bull.* **114**, 754–768 (2002).

16. Jones, C. H., Farmer G. L. & Unruh, J. Tectonics of Pliocene delamination of lithosphere of the Sierra Nevada, California. *Geo. Soc. Am. Bull.*, submitted (2004).
17. Dueker, K. G. & Sheehan A. F. Mantle discontinuity structure from mid-point stacks of converted *P* to *S* waves across the Yellowstone hotspot track. *J. Geophys. Res.* **102**, 8313–8327 (1997).
18. Kind, R. *et al.* Comprehensive seismic images of the crust and upper mantle beneath Tibet. *Science* **298**, 1219–1222 (2002).
19. Gilbert, H. J., Sheehan, A. F., Dueker, K. G. & Molnar P. Receiver functions in the western United States, with implications for upper mantle structure and dynamics, *J. Geophys. Res.* **108**(B5), 2229, DOI 10.1029/2001JB001194 (2003).
20. Fliedner, M., Klemperer, S. L. & Christensen, N. I. Three-dimensional seismic model of the Sierra Nevada arc, California, and its implications for crustal and upper mantle composition. *J. Geophys. Res.* **105**, 10899–10921 (2000).
21. Zhu, L. & Kanamori, H. Moho depth variation in southern California from teleseismic receiver functions. *J. Geophys. Res.* **105**, 2969–2980 (2000).
22. Bostock, M. G., Hyndman, R. D., Rondenay, S. & Peacock, S. M. An inverted continental Moho and serpentization of the forearc mantle. *Nature* **417**, 536–538 (2002).
23. Jones, C. H. & Phinney, R. A. Seismic structure of the lithosphere from teleseismic converted arrivals observed at small arrays in the southern Sierra Nevada and vicinity, California. *J. Geophys. Res.* **103**, 10065–10090 (1998).
24. Saleeby, J. & Foster, Z. Topographic response to mantle lithosphere removal in the southern Sierra Nevada region, California. *Geology* **37**, 245–248 (2004).
25. Liu, M. & Shen, Y. Q. Sierra Nevada uplift: A ductile link to mantle upwelling under the basin and range province. *Geology* **26**(4), 299–302 (1998).

26. Furlong, K. P. & Govers, R. Ephemeral crustal thickening at a triple junction: The Mendocino crustal conveyor. *Geology* **27**, 127–130 (1998).
27. Neil, E.A. & Houseman, G.A. Rayleigh-Taylor instability of the upper mantle and its role in intraplate orogeny. *Geophys. J. Int.* **138**, 89–107 (1999).
28. Houseman, G., Neil, E. A. & Kohler, M.D. Lithospheric instability beneath the Transverse Ranges of California *J. Geophys. Res.* **105**, 16237–16250 (2000).
29. Schott, B. & Schmeling, H. Delamination and detachment of a lithospheric root, *Tectonophysics* **296**, 225–247 (1998).
30. Pysklywec, R. N., Beaumont, C. & Fullsack, P. Lithospheric deformation during the early stages of continental collision: Numerical experiments and comparison with South Island, New Zealand. *J. Geophys. Res.* **107**(B7), DOI 10.1029/2001JB000252 (2002).
31. Bindschadler, D. L. & Parmentier, E. M. Mantle flow tectonics: The influence of a ductile lower crust and implications for the formation of topographic uplands on Venus. *J. Geophys Res.* **95**(B13), 21329–21344 (1990).
32. Davis, G. H. & Reynolds, S. J. *Structural Geology of Rocks and Regions*, 2nd Ed. (John Wiley & Sons, New York, 1996).
33. Zimmerman, M. E. & Kohlstedt, D. L. Melt segregation and LPO in anorthite-basalt deformed in torsion. *Eos Trans. AGU* **84**(46), Fall Meet. Suppl., Abstr. S22E–06 (2003).
34. Wernicke, B. P. Cenozoic extensional tectonics of the U.S. Cordillera, in *The Geology of North America Vol. G-3, The Cordilleran Orogen: Conterminous US.* (eds. Burchfiel, B. C., Lipman, P. W. & Zoback, M. L.) 553–581 (Geological Society of America, Boulder, Colorado, 1992).

35. Houseman, G. A. & Molnar, P. Gravitational (Rayleigh–Taylor) instability of a layer with non-linear viscosity and convective thinning of continental lithosphere. *J. Geophys. Res.* **128**, 125–150 (1997).
36. Schott, B., Yuen, D. A. & Schmeling, H. Viscous heating in heterogeneous media as applied to the thermal interaction between crust and mantle. *Geophys. Res. Lett.* **26**, 513–516 (1999).
37. Park, S. K., Hirasuna, B., Jiracek, G. R. & Kinn, C. L. Magnetotelluric evidence of lithospheric mantle thinning beneath the southern Sierra Nevada. *J. Geophys. Res.* **101**, 16241–16255 (1996).
38. Saltus, R. W. & Lachenbruch, A. H. Thermal evolution of the Sierra Nevada: Tectonic implications of new heat flow data. *Tectonics* **10**(2), 325–344 (1991).
39. Dumitru, T. A. Subnormal Cenozoic geothermal gradients in the extinct Sierra Nevada magmatic arc: Consequences of Laramide and post-Laramide shallow-angle subduction. *J. Geophys. Res.* **95**, 4925–4942 (1990).
40. House, M. A., Farley, K. F., Wernicke, B. P. & Dumitru, T.A. Cenozoic thermal evolution of the central Sierra Nevada from (U–Th)/He thermochronology. *Earth Planet. Sci. Lett.* **151**, 167–179 (1997).
41. Dickinson, W. R. The Basin and Range Province as a composite extensional domain. *Int. Geol. Rev.* **44**, 1–38 (2002).
42. Atwater, T. & Stock, J. Pacific-North America plate tectonics of the Neogene southwestern United States: An update. *Int. Geol. Rev.* **40**, 575–402 (1998).
43. Molnar, P. & Jones, C. H. A test of laboratory-based rheological parameters of olivine from an analysis of late Cenozoic convective removal of mantle lithosphere beneath the Sierra Nevada, California, USA. *Geophys. J. Int.*, submitted (2003).

44. Zandt, G. The southern Sierra Nevada drip and the mantle wind direction beneath the southwestern United States. *Int. Geol. Rev.* **45**, 213–224 (2003).
45. Furlong, K. P., Lock, J., Guzowski, C., Whitlock, J. & Benz, H. The Mendocino crustal conveyor: Making and breaking the California crust, in *The Lithosphere of Western North America and its Geophysical Characterization, The George A. Thompson Volume, International Book Series, Vol. 7* (eds. Klemperer, S. L. & Ernst, W. G.) 92–104 (Bellwether Publishing Ltd. for the Geological Society of America, Boulder, Colorado, 2003).
46. Hartog, R. & Schwartz, S. Y. Subduction induced strain in the upper mantle east of the Mendocino triple junction, California. *J. Geophys. Res.* **105**, 7909–7930 (2000).
47. Lange, R. A., Carmichael, I. S. E. & Renne, P. R. Potassic volcanism near the Mono basin, California: Evidence for high water and oxygen fugacities inherited from subduction. *Geology* **21**, 949–952 (1993).
48. Saleeby, J. B. Segmentation of the Laramide slab – Evidence from the southern Sierra Nevada region. *Geol. Soc. Am. Bull.* **115**(6), 655–668 (2003).

Supplementary information is available on *Nature's* World-Wide Web site (<http://www.nature.com>) or as paper copy from the London editorial office of *Nature*.

Acknowledgements GZ, HG, TJO, and CHJ cooperated on the seismology analysis and interpretation. MD and JS provided the geologic and tectonic context. CHJ led the PASSCAL deployment to collect the data. GZ wrote the paper with contributions from all the authors. GZ thanks George Gehrels, Paul Kapp, and Brad Hacker for comments on preliminary interpretations and manuscripts.

Competing interests statement The authors declare that they have no competing financial interests.

Correspondence and requests for materials should be addressed to G. Zandt (e-mail: zandt@geo.arizona.edu).

Figure legends

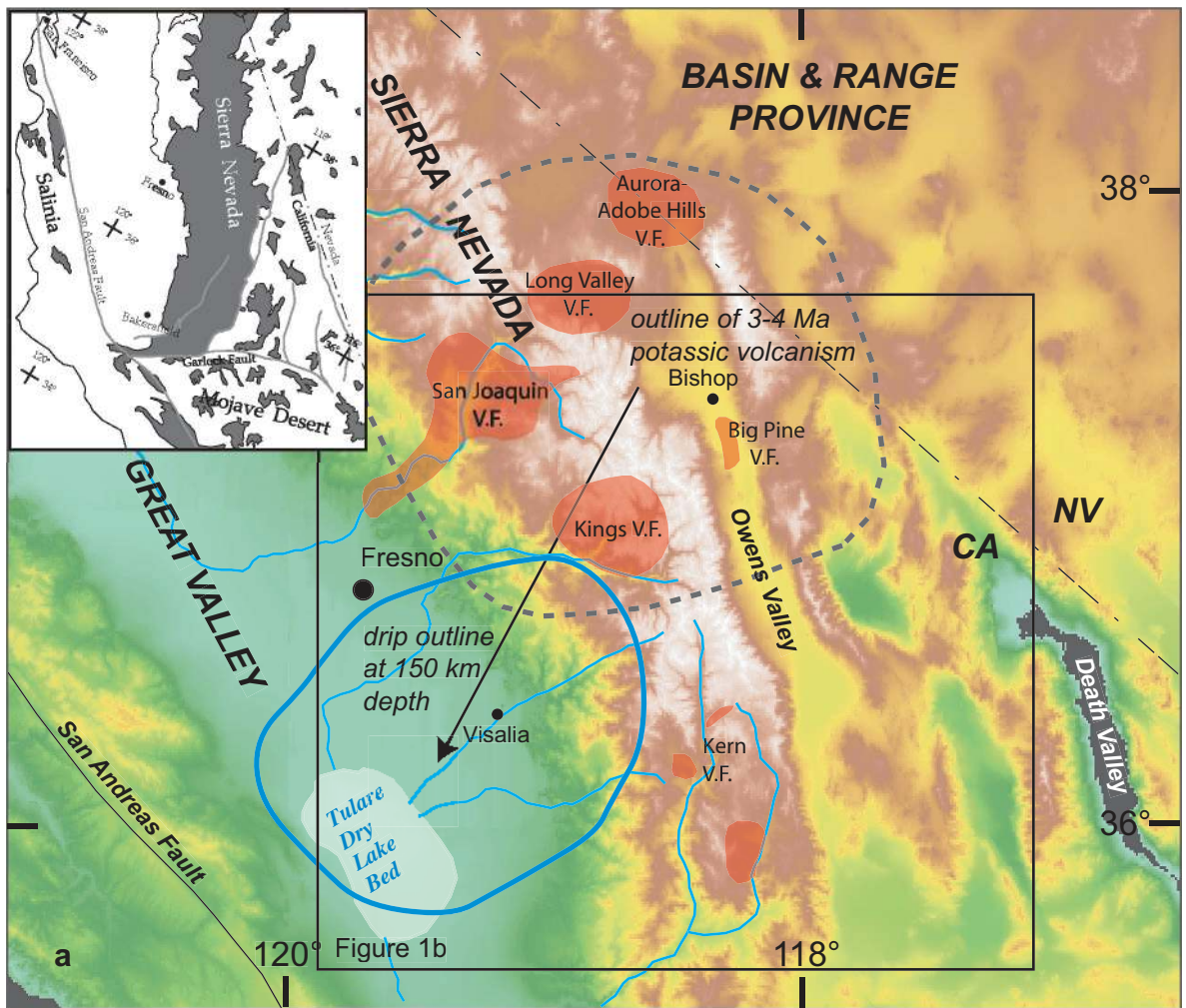
Figure 1 Map of study area illustrating topography and drainage patterns, Cenozoic volcanic fields^{15,16,46}, outline of 3–4 Ma potassic volcanism¹⁴, and outline of the mantle drip at 150-km depth¹³. Locations of broadband seismic stations used in this study are marked with symbols and station codes, indicating the presence and direction (short red dash) of lower-crustal anisotropy, absence of anisotropy (black +), or presence of some but differently oriented anisotropy (blue +). Orientation of the dash is along the slow-wavespeed direction and perpendicular to the fabric orientation. Small open circles locate small arrays used in an earlier receiver function study²³. Thick black lines are contours of Moho depths (in km) estimated from stacked receiver functions. Thin black line with blue transparency outlines region with no Moho arrival in the stacked receiver functions that is interpreted as a Moho hole (see text for further explanation). Three cross sections (A-A', B-B', C-C') are shown in Fig. 2. Inset shows distribution of granitoid batholithic rocks in the Sierra Nevada, Mojave Desert, and the Salinian terrane.

Figure 2 Cross sections through the 3D model of stacked receiver functions migrated into the depth domain and associated topography. Red areas represent large positive amplitudes (increase in wavespeed with depth), and blue areas represent negative amplitudes (decrease in wavespeed with depth). Hachure beneath prominent blue layers in crust represents east-dipping planar fabric producing seismic anisotropy. The V-shaped Moho holes are discussed in the text.

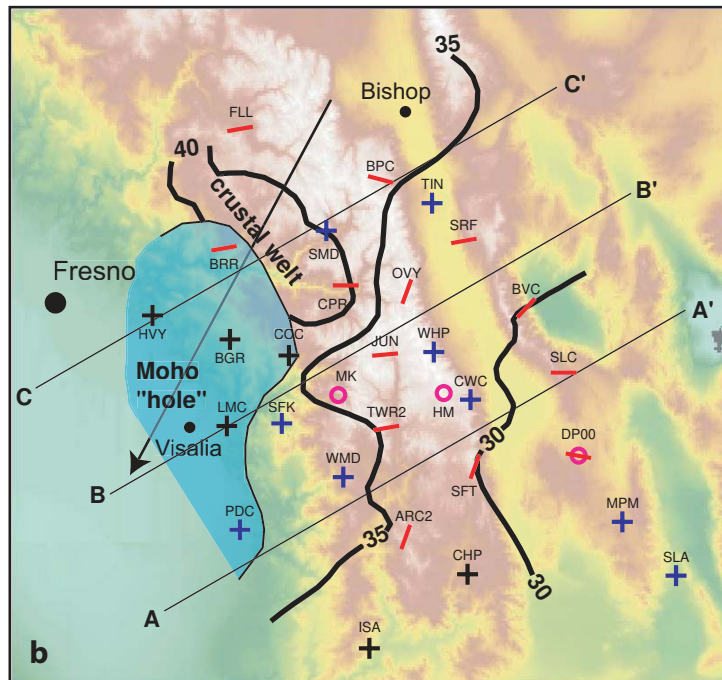
Figure 3 Synthetic stacked receiver function cross sections generated with a finite-difference wave-propagation technique for the seismic model shown

beneath the images. The synthetic data were processed with station and bin spacings similar to those used with the Southern Sierra Nevada data.

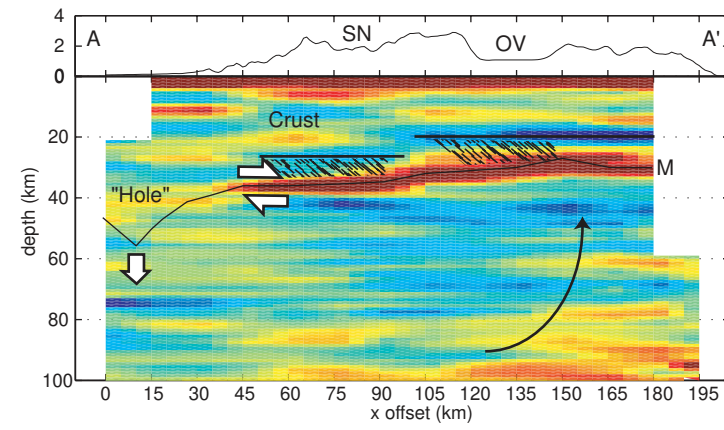
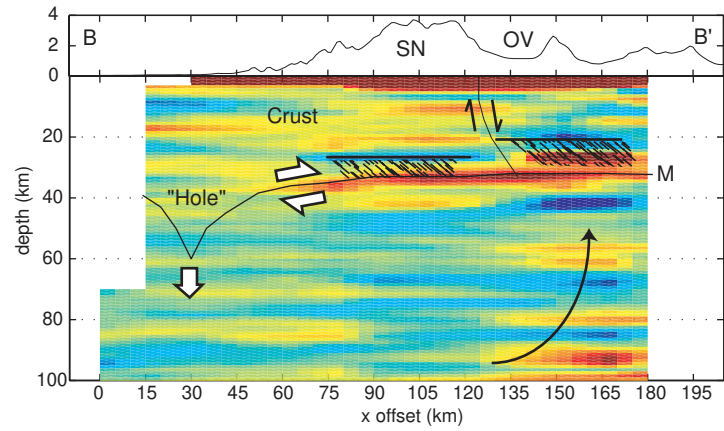
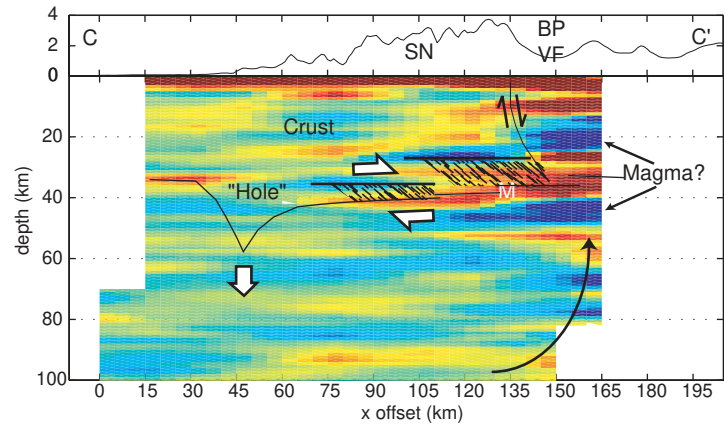
Figure 4 A sequential history of the foundering of the ultramafic root of the southern Sierra Nevada batholith. The proposed sequence is discussed in the text.



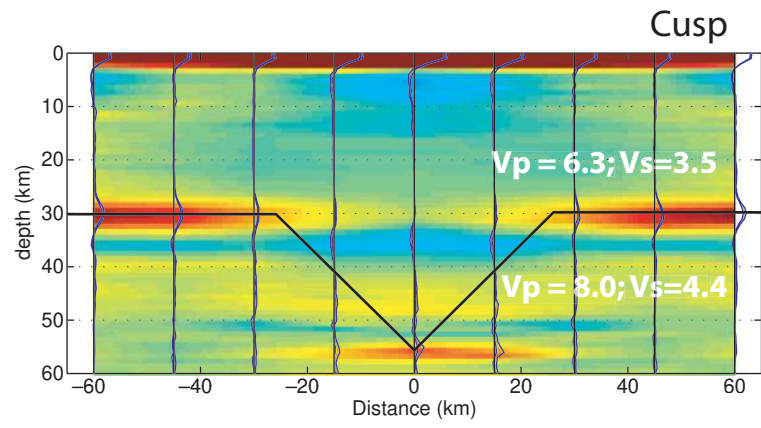
Zandt et al. Figure 1a MS #2004-02-15545



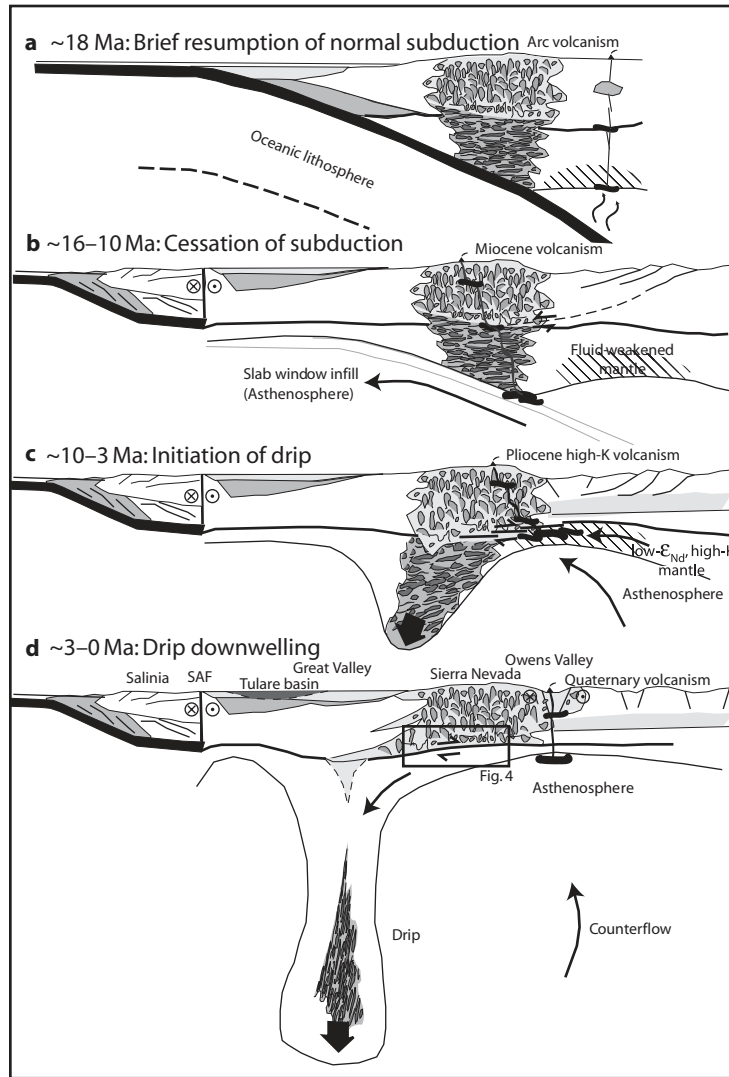
Zandt et al. Figure 1b MS #2004-02-15545



Zandt et al. Figure 2 MS #2004-02-15545



Zandt et al. Figure 3 MS #2004-02-15545



Zandt et al. Figure 4 MS #2004-02-15545